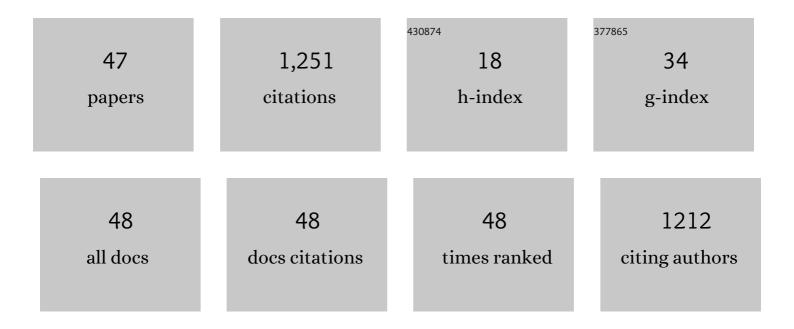
Changiz Dehghanian

List of Publications by Year in descending order

Source: https://exaly.com/author-pdf/11754323/publications.pdf Version: 2024-02-01



#	Article	IF	CITATIONS
1	Effects of spheroidization heat treatment and intercritical annealing on mechanical properties and corrosion resistance of medium carbon dual phase steel. Materials Chemistry and Physics, 2021, 257, 123721.	4.0	14
2	Silane coatings modified with hydroxyapatite nanoparticles to enhance the biocompatibility and corrosion resistance of a magnesium alloy. RSC Advances, 2021, 11, 26127-26144.	3.6	19
3	In- vitro corrosion behavior of the cast and extruded biodegradable Mg-Zn-Cu alloys in simulated body fluid (SBF). Journal of Magnesium and Alloys, 2021, 9, 2078-2096.	11.9	38
4	Tempering kinetics and corrosion resistance of quenched and tempered AISI 4130 medium carbon steel. Materials and Corrosion - Werkstoffe Und Korrosion, 2021, 72, 1808-1812.	1.5	7
5	Processing Route Effects on the Mechanical and Corrosion Properties of Dual Phase Steel. Metals and Materials International, 2020, 26, 882-890.	3.4	24
6	Unraveling the Effect of Martensite Volume Fraction on the Mechanical and Corrosion Properties of Low arbon Dualâ€Phase Steel. Steel Research International, 2020, 91, 1900327.	1.8	13
7	Effects of tempering on the mechanical and corrosion properties of dual phase steel. Materials Today Communications, 2020, 22, 100745.	1.9	19
8	Effect of grain size on the corrosion resistance of low carbon steel. Materials Research Express, 2020, 7, 016522.	1.6	39
9	Thermodynamics basis of saturation of martensite content during reversion annealing of cold rolled metastable austenitic steel. Vacuum, 2020, 174, 109220.	3.5	12
10	Significance of Martensite Reversion and Austenite Stability to the Mechanical Properties and Transformation-Induced Plasticity Effect of Austenitic Stainless Steels. Journal of Materials Engineering and Performance, 2020, 29, 3233-3242.	2.5	29
11	Effect of electrodeposition parameters and substrate on morphology of Si-HA coating. Surface and Coatings Technology, 2019, 375, 341-351.	4.8	30
12	Phase transformation mechanism and kinetics during step quenching of st37 low carbon steel. Materials Research Express, 2019, 6, 1165f2.	1.6	10
13	The Microstructure, and Mechanical and Corrosion Properties of As-Cast and As-Extruded Mg-2%Zn-x%Cu Alloys After Solution and Aging Heat Treatments. Journal of Materials Engineering and Performance, 2019, 28, 2305-2315.	2.5	14
14	Flower-like mesoporous nano NiCo2O4 -decorated ERGO/Ni-NiO foam as electrode materials for supercapacitor. Materials Research Bulletin, 2019, 109, 10-20.	5.2	11
15	Synthesis of nanoporous copper foam-applied current collector electrode for supercapacitor. Journal of the Iranian Chemical Society, 2019, 16, 283-292.	2.2	18
16	Influence of Near-Surface Severe Plastic Deformation of Mild Steel on the Inhibition Performance of Sodium Molybdate and 1H-Benzotriazole in Artificial Sea Water. Journal of Materials Engineering and Performance, 2018, 27, 550-559.	2.5	4
17	Characterization of silicon- substituted nano hydroxyapatite coating on magnesium alloy for biomaterial application. Materials Chemistry and Physics, 2018, 203, 27-33.	4.0	37
18	In vitro degradation and cytotoxicity of Mg-5Zn-0.3Ca/nHA biocomposites prepared by powder metallurgy. Transactions of Nonferrous Metals Society of China, 2018, 28, 1745-1754.	4.2	21

#	Article	IF	CITATIONS
19	Pulsed electrodeposition of reduced graphene oxide on Ni NiO foam electrode for high-performance supercapacitor. International Journal of Hydrogen Energy, 2018, 43, 12233-12250.	7.1	18
20	Facile synthesis of nano dendrite-structured Ni–NiO foam/ERGO by constant current method for supercapacitor applications. Journal of Applied Electrochemistry, 2018, 48, 923-935.	2.9	12
21	Preparation of dendritic nanoporous Ni-NiO foam by electrochemical dealloying for use in high-performance supercapacitors. Journal of Solid State Electrochemistry, 2018, 22, 3639-3645.	2.5	6
22	Corrosion inhibition of copper, mild steel and galvanically coupled copper-mild steel in artificial sea water in presence of 1H-benzotriazole, sodium molybdate and sodium phosphate. Corrosion Science, 2017, 126, 272-285.	6.6	91
23	Effect of duty cycle and electrolyte additive on photocatalytic performance of TiO2-ZrO2 composite layers prepared on CP Ti by micro arc oxidation method. Surface and Coatings Technology, 2016, 307, 554-564.	4.8	25
24	The Correlation Among Deposition Parameters, Structure and Corrosion Behavior in ZnNi/Nano-SiC Coating. Journal of Materials Engineering and Performance, 2016, 25, 3746-3755.	2.5	3
25	Synthesis, characterization and electrochemical performance of a new imidazoline derivative as an environmentally friendly corrosion and scale inhibitor. Research on Chemical Intermediates, 2016, 42, 4551-4568.	2.7	13
26	Electrochemical assessment of characteristics and corrosion behavior of Zr-containing coatings formed on titanium by plasma electrolytic oxidation. Surface and Coatings Technology, 2015, 279, 79-91.	4.8	16
27	Corrosion protection of the reinforcing steels in chloride-laden concrete environment through epoxy/polyaniline–camphorsulfonate nanocomposite coating. Corrosion Science, 2015, 90, 239-247.	6.6	110
28	In situ synthesis of polyaniline–camphorsulfonate particles in an epoxy matrix for corrosion protection of mild steel in NaCl solution. Corrosion Science, 2014, 85, 204-214.	6.6	114
29	Deposition and characterization of nanocrystalline and amorphous Ni–W coatings with embedded alumina nanoparticles. Ceramics International, 2013, 39, 7759-7766.	4.8	37
30	Influence of heat treatment temperature on the electrochemical properties and corrosion behavior of RuO2-TiO2 coating in acidic chloride solution. Protection of Metals and Physical Chemistry of Surfaces, 2013, 49, 699-704.	1.1	8
31	THE INFLUENCE OF GRAIN SIZE OF PURE IRON METAL ON CORROSION INHIBITION IN PRESENCE OF SODIUM NITRITE. International Journal of Modern Physics Conference Series, 2012, 05, 793-800.	0.7	4
32	Corrosion behavior of Ni–P/nano-TiC composite coating prepared in electroless baths containing different types of surfactant. Progress in Natural Science: Materials International, 2012, 22, 480-487.	4.4	43
33	Studying the effects of the addition of TiN nanoparticles to Ni–P electroless coatings. Applied Surface Science, 2011, 258, 1876-1880.	6.1	55
34	Comparison of the coating properties and corrosion rates in electroless Ni–P/PTFE composites prepared by different types of surfactants. Applied Surface Science, 2011, 257, 8653-8658.	6.1	102
35	Electrochemical polarization and passivation of nanostructured iron in acid solution. Anti-Corrosion Methods and Materials, 2010, 57, 142-147.	1.5	4
36	The effect of grain size on the corrosion inhibitor adsorption of nanocrystalline iron metal. International Journal of Materials Research, 2010, 101, 366-371.	0.3	3

CHANGIZ DEHGHANIAN

#	Article	IF	CITATIONS
37	Inhibitor effect of sodium benzoate on the corrosion behavior of nanocrystalline pure iron metal in near-neutral aqueous solutions. Journal of Solid State Electrochemistry, 2010, 14, 1855-1861.	2.5	17
38	The influence of nanocrystalline state of iron on the corrosion inhibitor behavior in aqueous solution. Journal of Applied Electrochemistry, 2010, 40, 1949-1956.	2.9	5
39	THE INFLUENCE OF PULSE PARAMETERS ON THE MICROSTRUCTURE OF IRON ELECTRODEPOSITS. International Journal of Nanoscience, 2010, 09, 365-370.	0.7	0
40	Surface Hardening of AISI H13 Steel Using Pulsed Plasma Electrolytic Carburizing (PPEC). Plasma Processes and Polymers, 2009, 6, S168.	3.0	12
41	Effects of grain size on the electrochemical corrosion behaviour of electrodeposited nanocrystalline Fe coatings in alkaline solution. Corrosion Science, 2009, 51, 1844-1849.	6.6	91
42	Wear and corrosion properties of nanocrystalline coatings on stainless steel produced by plasma electrolytic nitrocarburizing. International Journal of Materials Research, 2008, 99, 92-100.	0.3	8
43	Corrosion properties of plasma electrolytic coated samples. Anti-Corrosion Methods and Materials, 2007, 54, 148-154.	1.5	9
44	Evaluation of Nanocrystalline Microstructure, Abrasion, and Corrosion Properties of Carbon Steel Treated by Plasma Electrolytic Boriding. Plasma Processes and Polymers, 2007, 4, S711-S716.	3.0	29
45	Nanocrystalline Structure Produced by Complex Surface Treatments: Plasma Electrolytic Nitrocarburizing, Boronitriding, Borocarburizing, and Borocarbonitriding. Plasma Processes and Polymers, 2007, 4, S721-S727.	3.0	45
46	Electrochemical Behavior of Steel in Salt Contaminated Concrete: Part 1. Corrosion, 1983, 39, 299-305.	1.1	3
47	Electrochemical Behavior of Steel in Concrete as a Result of Chloride Diffusion into Concrete: Part 2. Corrosion, 1982, 38, 494-499.	1.1	9